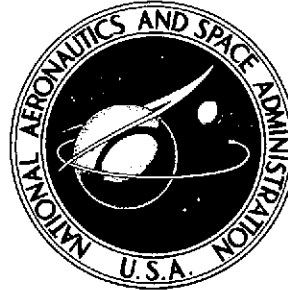


14p

NASA TECHNICAL NOTE



NASA TN D-7618

NASA TN D-7618

(NASA-TN-D-7618) AN ADVERSE EFFECT OF  
FILM COOLING ON THE SUCTION SURFACE OF A  
TURBINE VANE (NASA) 27 p HC \$3.00  
26

N74-20593

CSCS 20M

Unclas  
34334

H1/33



AN ADVERSE EFFECT OF FILM COOLING  
ON THE SUCTION SURFACE  
OF A TURBINE VANE

*by Herbert J. Gladden and James W. Gauntner*

*Lewis Research Center*

*Cleveland, Ohio 44135*



1. Report No. NASA TN D-7618	2. Government Accession No.	3. Recipient's Catalog No.	
4. Title and Subtitle AN ADVERSE EFFECT OF FILM COOLING ON THE SUCTION SURFACE OF A TURBINE VANE		5. Report Date APRIL 1974	6. Performing Organization Code
		8. Performing Organization Report No. E-7744	
7. Author(s) Herbert J. Gladden and James W. Gauntner		10. Work Unit No. 501-24	11. Contract or Grant No.
9. Performing Organization Name and Address Lewis Research Center National Aeronautics and Space Administration Cleveland, Ohio 44135		13. Type of Report and Period Covered Technical Note	
		14. Sponsoring Agency Code	
12. Sponsoring Agency Name and Address National Aeronautics and Space Administration Washington, D. C. 20546		15. Supplementary Notes	
16. Abstract Film-cooling-air ejection from the suction surface of a turbine vane was investigated. This investigation was conducted in a four-vane cascade on a J75 size turbine vane which had a row of holes near the leading edge. The experimental data are presented herein. It was found that a small amount of film-cooling air had a detrimental effect on the downstream vane wall cooling effectiveness. It was also shown that the presence of the film-cooling holes, without blowing, also caused an increase in vane wall temperatures. These results came from an increase in the gas-side heat transfer coefficient that was apparently caused by a laminar or transitional boundary layer becoming transitional or turbulent.			
17. Key Words (Suggested by Author(s)) Film cooling Heat transfer Turbine vane		18. Distribution Statement Unclassified - unlimited Category 33  Cat. 33	
19. Security Classif. (of this report) Unclassified	20. Security Classif. (of this page) Unclassified	21. No. of Pages <del>25</del> 26	22. Price* \$3.00

\* For sale by the National Technical Information Service, Springfield, Virginia 22151

# AN ADVERSE EFFECT OF FILM COOLING ON THE SUCTION SURFACE OF A TURBINE VANE

by Herbert J. Gladden and James W. Gauntner

Lewis Research Center

## SUMMARY

The effects of film-cooling-air ejection from the suction surface of a turbine vane were investigated. This investigation was conducted in a four-vane cascade on a J75 size turbine vane which had a single row of holes on the suction surface. The experimental data are presented herein.

The film-cooling-air ejection and, also, the film-cooling holes alone had a detrimental effect on the downstream cooling effectiveness. There was some indication that these results were accumulative. Under certain conditions, the heat transfer coefficients increased, apparently because a laminar or transitional boundary layer became transitional or turbulent.

The test conditions investigated were gas temperature and pressures of 1260 K (1800° F) and 22.7 to 45.5 N/cm<sup>2</sup> (33 to 66 psia), a coolant temperature of 280 K (50° F), midchord-convection coolant- to gas-flow ratios of 0.0 to 0.056, and film-cooling- to gas-flow ratios from 0.0 to 0.028. The film-cooling flow range corresponds to film-coolant- to main-stream-blowing ratios of 0.0 to 2.07.

## INTRODUCTION

The effects of film-cooling-air ejection from a single row of holes in the suction surface of a turbine vane were investigated. Particular attention was given to the effects on the downstream wall temperatures of the ejected air and of the film-cooling holes.

For certain combinations of turbine inlet temperature and pressure, laminar or transitional flow may exist over all, or a portion of, the suction surface of turbine vanes. The injection of film-cooling air into the boundary layer may result in an increased gas-side heat transfer coefficient at downstream locations on the vane surface. Therefore, in certain instances, the benefits derived from film cooling are not sufficient to counter-

balance the effect of increased gas-side heat transfer coefficients. Experimental results presented in references 1 to 3 indicate that, under certain conditions, film-cooling-air ejection resulted in decreased cooling effectiveness. Reference 4 discusses the effect of holes, without blowing, on the gas-side heat transfer coefficient.

In order to investigate these adverse effects in more detail, a control experiment to demonstrate film cooling effects on the suction surface was performed. Preliminary results of this investigation are presented in reference 5. The film-cooled test vane used in this investigation had a row of film-cooling holes near the leading edge. Vane metal temperatures were measured both with and without blowing to determine the effects of the ejected air. Vane metal temperatures were also measured with and without film-cooling holes to determine the effect of the holes alone. A comparison of these wall temperatures was made by means of a temperature difference ratio. This investigation was conducted in a four-vane cascade.

The following test conditions were used:

Gas inlet total temperature, K ( <sup>o</sup> F) . . . . .	1260 (1800)
Gas inlet total pressure, N/cm <sup>2</sup> (psia) . . . . .	22.7, 25.5, 31.0, 45.5 (33.0, 37.0, 45.0, 66.0)
Fuel-air ratio . . . . .	0.022
Coolant inlet temperature, K ( <sup>o</sup> F) . . . . .	280 (50)
Midchord-convection-coolant- to gas-flow ratios . . . . .	0.0 to 0.056
Film-coolant- to gas-flow ratios . . . . .	0.0 to 0.028
Film-coolant- to main-stream-blowing ratios . . . . .	0.0 to 2.07

Although both the International System of Units (SI) and the U. S. customary system of units are used in this report, the work was actually done in U. S. customary units. Conversion to the SI system was for reporting purposes only.

## APPARATUS

### Cascade Description

A detailed description of the cascade facility is given in reference 6. The test section was a 23<sup>o</sup> annular sector of a stator row and contained four vanes and five flow channels. A plan view of the test section is shown in figure 1. The central flow channel was formed by the suction surface of vane 2 and the pressure surface of vane 3. The two outer vanes in the cascade completed the flow channels for the two central vanes and also served as radiation shields between these vanes and the water-cooled cascade walls.

The test vane (vane 2) had two separate cooling-air systems, one for the film-

cooling flow, and the second for the midchord convection flow. The cooling-air flow rates were metered by turbine-type flowmeters. The lower 10 percent of the film-cooling-airflow range was metered by a hot-wire anemometry system.

### Vane Description

A J75 size vane which had a span of 9.78 centimeters (3.85 in.) and a chord of 6.28 centimeters (2.47 in.) was used in this investigation. The vane material was MAR M 302. The internal cooling configuration, shown in figures 2(a) and (b), consisted of an impingement-cooled midchord region and a pin-fin-augmented convection-cooled trailing-edge region. This vane was designed to have an impingement-cooled leading edge. However, for this investigation, the leading-edge impingement tube was removed, and the chamber was blocked at the tip end. Therefore, the cooling air entering the vane from the tip plenum (fig. 2(b)) was restricted to cooling the midchord and trailing-edge regions only. The leading-edge chamber served as a plenum for the film-cooling holes which were added to the vane after the initial series of tests. The film-cooling air entered the plenum at the vane hub.

The film-cooled version of the test vane had 57 film-cooling holes located on the suction surface 2.11 centimeters (0.83 in.) downstream of the leading-edge stagnation point. These film-cooling holes had centers equally spaced 0.157 centimeter (0.062 in.) apart and had a diameter of 0.064 centimeter (0.025 in.). They were angled at  $28^{\circ}$  with respect to a line tangent to the suction surface at the location of the holes.

The midchord supply tube contained a staggered array of 0.038-centimeter (0.015-in.) diameter holes. There were 481 and 334 holes, respectively, on the suction and pressure surface. The midspan chordwise center-to-center hole spacing was 0.24 and 0.28 centimeter (0.095 and 0.110 in.), and the spanwise center-to-center hole spacing was 0.20 and 0.23 centimeter (0.080 and 0.092 in.), respectively, on the suction and pressure surfaces. The hole-to-impingement-surface spacing was 0.076 centimeter (0.030 in.) (two hole diameters).

The split trailing edge contained four rows of oblong pin fins and a single row of round pin fins. The oblong pin fins were 0.38 centimeter (0.15 in.) by 0.25 centimeter (0.10 in.) and varied in height from 0.18 to 0.094 centimeter (0.070 to 0.037 in.). The round pin fins had a diameter of 0.20 centimeter (0.080 in.) and a height of 0.064 centimeter (0.025 in.).

### INSTRUMENTATION

Eight Chromel-Alumel thermocouples were located at the midspan (fig. 2(a)) on the

suction surface of the test vane and adjacent to the central flow channel of the cascade. The location of the thermocouples and the thickness of the vane wall are given in table I. All symbols are defined in the appendix. The construction and installation of the thermocouples is discussed in reference 7. The cooling-air temperature and pressure were measured at the inlet to the vanes. The combustion gas inlet conditions were measured by spanwise traversing probes. These and other operational instrumentation are discussed in reference 6.

## ANALYSIS METHODS

The local cooling effectiveness  $\phi$  (also called temperature difference ratio) is defined by equation (1).

$$\phi = \frac{T_{g,e} - T_w}{T_{g,e} - T_c} \quad (1)$$

Reference 5 shows that  $\phi$  can be correlated as a function of the film-coolant- to gas-flow ratio  $w_{fc}/w_g$  for a constant midchord-coolant- to gas-flow ratio  $w_{mc}/w_g$ . This method was used herein to examine the effect of the film-cooling-air ejection on the overall cooling effectiveness  $\phi$ .

Reference 8 shows that  $\phi$  can also be correlated as a function of the midchord-coolant- to gas-flow ratio. This method was used herein to compare the experimental data with film-cooling holes (without blowing) and the data without film-cooling holes.

A two-dimensional heat balance was made on an element of the vane wall. The assumptions were (1) the temperature drop through the wall was negligible, (2) the spanwise conduction was negligible, and (3) there was no heat transfer between the pressure and suction surfaces. With these assumptions, the following equation was developed to compare the relative magnitude of the gas-side heat transfer coefficient with and without film-cooling holes:

$$h_g(T_{g,e} - T_w) = h_c(T_w - T_c) - k_w t \frac{d^2 T_w}{dx^2} \quad (2)$$

This equation was solved for the effective coolant-side heat transfer coefficient without holes  $h_{c,00}$  and then equated to that with holes but without blowing  $h_{c,0}$ . These heat transfer coefficients were equal because the midchord convection flow rates were equal

and the temperature effects on properties were negligible. The resulting equation was solved for  $h_{g,o}/h_{g,oo}$ .

$$\frac{h_{g,o}}{h_{g,oo}} = \frac{\left(\frac{T_w - T_c}{T_{g,e} - T_w}\right)_o}{\left(\frac{T_w - T_c}{T_{g,e} - T_w}\right)_{oo}} + \frac{k_w t}{h_{g,oo} \left(T_{g,e} - T_w\right)_o} \left[ \frac{d^2 T_{w,oo}}{dx^2} \frac{(T_w - T_c)_o}{(T_w - T_c)_{oo}} - \frac{d^2 T_{w,o}}{dx^2} \right] \quad (3)$$

For simplification of the calculation procedure, it was further assumed that the gas and coolant temperatures could be replaced by their respective inlet values. The second derivative of the wall temperature with respect to vane chordwise surface distance was obtained by numerically differentiating the experimental data at the point of interest. The value of thermal conductivity  $k_w$  of MAR M 302 was taken from reference 9.

The gas-side heat transfer coefficients for both turbulent and transitional boundary layers were calculated by the formulation of Ambrok (eq. (9) of ref. 10). This formulation was modified by a ratio of the static gas temperature to the wall temperature raised to the 1/4 power to account for the property variation across the boundary layer as suggested by Kays (ref. 11). For laminar boundary layers, the gas-side heat transfer coefficient was based on the work of Brown and Donoughe (ref. 12) and corrected for variable wall temperature by the results of reference 13. Transition from laminar flow was assumed to occur at the location which had a momentum-thickness Reynolds number of 200 (ref. 14). Transition to turbulent flow was assumed to occur at the location which had a momentum-thickness Reynolds number of 360 (ref. 11). The gas-side heat transfer coefficients required in equation (3) and calculated by these methods are shown in figure 3 for three gas inlet pressures. The laminar, transition, and turbulent regions are noted in the figure. Based on the Reynolds number range of 200 to 360, laminar flow persisted downstream of the film-cooling holes for only the low-gas-pressure (22.7 N/cm<sup>2</sup> (33 psia)) case. These heat transfer coefficients were calculated for the vane without film-cooling flow and without film-cooling holes.

Used in the calculation of the gas-side heat transfer coefficient was the vane midspan experimental surface-static-pressure distribution for the test vane, shown in figure 4. These data, taken from reference 15, were for the design exit Mach number of 0.85. The data are presented as a surface-static-pressure to inlet-total-pressure ratio and are plotted as a function of the dimensionless surface distance  $x/L$ . The figure shows that a favorable pressure gradient existed in the region between the film-cooling holes and an  $x/L$  of 0.63. An adverse pressure gradient existed between this point and the trailing edge.

## TEST PROCEDURE

The average gas inlet total temperature and the midspan exit Mach number were maintained at 1260 K (1800° F) (fuel-air ratio of 0.022) and 0.085, respectively. The effects of gas-side Reynolds number were examined by taking data at four gas inlet-total-pressure levels: 22.7, 25.5, 31.0, and 45.5 N/cm<sup>2</sup> (33, 37, 45, and 66 psia). Ambient-temperature cooling air was used for both the midchord convection-side airflow and the film-cooling airflow.

The first series of tests were made at 31 N/cm<sup>2</sup> (45 psia) and without film-cooling holes on the vane. The midchord-coolant- to gas-flow ratio  $w_{mc}/w_g$  for these tests was varied in a stepwise fashion from 0.0 to about 0.056.

A single row of film-cooling holes near the leading-edge suction surface of the test vane were provided for the second series of tests. Film-cooling data were taken at each of the preceding pressures and at selected midchord-coolant-flow ratios. The film-cooling flow ratio  $w_{fc}/w_g$  was varied from 0.0 to about 0.028, which corresponded to a film-coolant- to mainstream-blowing ratio of 0.0 to 2.07.

## RESULTS AND DISCUSSION

The effects of film-cooling airflow from a single row of holes in the suction surface of a turbine vane were investigated. The data from this investigation are presented in table II. An adverse effect on the cooling effectiveness, caused by cooling-air injection into the boundary layer, was noted on the aft 60 percent of the suction surface (thermocouples 1 to 6, fig. 2(a)). That is, the vane wall temperatures increased with the introduction of the film coolant. This effect was not noticed in the midchord region near the film-cooling holes at thermocouple 7. An adverse effect was also noted which was attributed to just the presence of the film-cooling holes. Two thermocouple locations were selected as typical to demonstrate these adverse effects (thermocouples 2 and 4, fig. 2(a)).

### Adverse Effect of Blowing

The effects of film-cooling-air ejection near the leading edge are graphically shown by a plot of the local cooling effectiveness  $\phi$  as a function of the film-coolant- to gas-flow ratio  $w_{fc}/w_g$ . These data are presented in figures 5(a) and (b) for thermocouples 2 and 4, respectively. The film-coolant flow ratio varied from 0 to 0.028. Representative values of the blowing ratio, defined as  $(\rho V)_{fc}/(\rho V)_g$ , are also included in the figures.



The midchord-convection-coolant- to gas-flow ratio  $w_{mc}/w_g$  is shown parametrically. The data shown were taken at a gas inlet total pressure of  $22.7 \text{ N/cm}^2$  (33 psia).

The cooling effectiveness  $\phi_o$  (with holes but no blowing) is shown by those data points on the ordinate. For data points near the ordinate, the cooling effectiveness  $\phi$  near the trailing edge rapidly decreased. A minimum value of  $\phi$  was reached at an  $w_{fc}/w_g$  of about 0.002. For film-coolant flows between zero and the point where  $\phi$  reached a minimum, the increase in gas-side heat transfer coefficient was greater than the increased benefits of film cooling. As a result the local cooling effectiveness decreased. Apparently, a small amount of film-cooling airflow caused a laminar or transitional boundary layer to become transitional or turbulent with the accompanying increase in the gas-side heat transfer coefficient. As  $w_{fc}/w_g$  increased beyond 0.002, the cooling effectiveness also increased.

The maximum change in wall temperature caused by the film-cooling-air ejection was found by using the initial and minimum temperature difference ratios and the gas and coolant temperatures investigated. The increases in the trailing-edge temperature from figures 5(a) and (b) for  $w_{mc}/w_g$  of 0.035 were 93 and 84 kelvins (168 and 151 deg F), respectively. For  $w_{mc}/w_g$  of 0.007, the increases in temperature were 87 and 66 kelvins (157 and 119 deg F), respectively.

As shown in figure 5, as the midchord-coolant-flow ratio  $w_{mc}/w_g$  increased (0.007 to 0.018 to 0.035), the film-coolant-flow ratio  $w_{fc}/w_g$  at which  $\phi$  equals its original value  $\phi_o$  (where  $w_{fc}/w_g$  is zero) also increased. The dot-dashed line in figure 5 connects the points where  $\phi$  equals  $\phi_o$ . Combinations of midchord-convection-coolant-flow ratios and film-coolant-flow ratios which occur to the right of the dot-dashed line represent beneficial film cooling relative to the vane with holes but without blowing. Combinations which occur to the left represent detrimental film cooling. Each thermocouple location, of course, has its own beneficial and detrimental regions.

Figure 5 has shown the effect of film cooling for a gas pressure of  $22.7 \text{ N/cm}^2$  (33 psia). Calculations indicate that this pressure and temperature correspond to a laminar and transitional gas-side boundary layer at the midspan. The effect of film cooling on higher gas-side pressures (higher Reynolds numbers) was also of interest. This effect is shown in figure 6, where the local cooling effectiveness  $\phi$  is plotted as a function of the film-coolant-flow ratio  $w_{fc}/w_g$  with the gas inlet total pressure as a parameter. Again, data on the ordinate represent the case of holes without blowing. The midchord-coolant-flow ratio  $w_{mc}/w_g$  for the data shown was about 0.035.

Inspection of the left sides of figures 6(a) and (b) indicates that as the gas pressure (Reynolds number) increased, the adverse effect of the film-cooling-air ejection was reduced until there appeared to be no adverse effect at a gas pressure of  $45.5 \text{ N/cm}^2$  (66 psia). At film-coolant-flow ratios  $w_{fc}/w_g$  higher than about 0.002, the local cooling effectiveness  $\phi$  for all pressure levels was similar. These phenomena suggest

that above a film-coolant-flow ratio  $w_{fc}/w_g$  of 0.002 and at thermocouples 2 and 4, the boundary layer had become fully turbulent for all pressure levels studied. As mentioned previously, small amounts of film-cooling air ejected near the leading edge have apparently tripped a laminar or transitional boundary layer to a transitional or turbulent boundary layer.

### Adverse Effect of Holes

The effect on the boundary layer of the presence of film-cooling holes without blowing was also of interest. This effect was noted by comparing the vane cooling effectiveness with and without film-cooling holes present. Figure 7 shows a plot of the local cooling effectiveness as a function of the midchord-coolant- to gas-flow ratio  $w_{mc}/w_g$  for both cases. The gas inlet pressure was  $31 \text{ N/cm}^2$  (45 psia). As noted in the figures, the cooling effectiveness was considerably higher without the film-cooling holes. This result demonstrates that the presence of film-cooling holes in the vane near the leading edge significantly altered the heat transfer characteristics near the vane trailing edge apparently by tripping the boundary layer.

Equation (3) has been used to show the effect of the holes on gas-side heat transfer coefficient. This effect is shown in figure 8 as a function of the distance from the leading-edge stagnation point. The results indicate that the increase in the heat transfer coefficient was also a function of the midchord-coolant-flow ratio  $w_{mc}/w_g$ , probably as a result of the assumptions used in the analysis.

The change in wall temperature due to the film-cooling holes was found by using the two local cooling effectiveness values from figure 7 at a given midchord-coolant-flow ratio and the measured gas and coolant temperatures. The increases in the trailing-edge temperature at thermocouples 2 and 4 due to the presence of holes were 117 and 88 kelvins (210 and 158 deg F), respectively, for  $w_{mc}/w_g$  of 0.035 and for a gas pressure of  $31 \text{ N/cm}^2$  (45 psia). Data are not available for similar calculations at other pressures.

### Adverse Effect of Holes and Blowing

The adverse effect on the cooling effectiveness has been discussed first with blowing at low and moderate pressures and then with holes alone at moderate pressure. A combination of these effects is shown in figure 9(a), where the local cooling effectiveness is plotted as a function of  $x/L$  for four cases at  $31 \text{ N/cm}^2$  (45 psia). Curve A represents the cooling effectiveness  $\phi_{00}$  for convection cooling only. With just the

addition of film-cooling holes near the leading edge, the cooling effectiveness  $\phi_0$  dropped substantially in the midchord and trailing-edge regions (curve B). When a small amount of blowing was introduced,  $w_{fc}/w_g$  equal to 0.0014, the cooling effectiveness was reduced even further (curve C). The lower two curves apparently represent a tripped boundary layer, in which the point of transition moves forward on the vane surface with increased disturbance near the leading edge. For substantial blowing the cooling effectiveness (curve D) never achieved those values which were obtained without film-cooling holes. Thus, at these conditions, the addition of film cooling had a detrimental effect on the trailing-edge region of the suction surface of this vane.

Experimental data without film-cooling holes are available for only the  $31 \text{ N/cm}^2$  (45 psia) case. However, it is of interest to speculate what effect the presence of the film-cooling holes would have at the other pressures investigated. For example, at  $45.5 \text{ N/cm}^2$  (66 psia), the boundary layer was determined to be turbulent in the trailing-edge region (fig. 3). Therefore, the presence of the holes would probably have little or no effect on the cooling effectiveness in the trailing-edge region. Inspection of the data indicates that there was no adverse effect between the case with holes only (no blowing) and the case with small amounts of blowing.

Figure 9(b) shows the local cooling effectiveness as a function of  $x/L$  for the two cases of film-cooling holes with blowing and without blowing at  $22.7 \text{ N/cm}^2$  (33 psia). As discussed previously, a substantial reduction in the cooling effectiveness occurred in the midchord and trailing-edge regions. The boundary layer was apparently tripped at this pressure by a small amount of blowing. The effect of the film-cooling holes was not studied at this pressure.

## SUMMARY OF RESULTS

An experimental investigation of the effects of film cooling on the suction surface of a turbine vane was made in a four-vane cascade. The film-cooling air was ejected near the leading edge. The results were as follows:

1. Ejection of film-cooling air, under certain conditions, resulted in increased vane wall temperatures at positions downstream from the point of ejection. For example, a small amount of film-cooling air (0.2 percent of the gas flow) resulted in downstream wall temperature increases as high as 93 kelvins (168 deg F). This effect was not observed in an apparently turbulent boundary layer. Evidently, a laminar or transitional boundary layer was tripped into a transitional or turbulent regime at the lower pressure levels investigated.

2. The presence of film-cooling holes without blowing near the leading edge also resulted in increased wall temperatures. These wall temperature increases were as high

as 117 kelvins (210 deg F). As before, the boundary layer apparently underwent a transition.

3. At a gas pressure of  $31 \text{ N/cm}^2$  (45 psia), the vane wall temperatures increased with the addition of film-cooling holes (no blowing) and increased further with small amounts of blowing. The adverse effects on the gas-side heat transfer coefficient were apparently accumulative.

4. Also at a gas pressure of  $31 \text{ N/cm}^2$  (45 psia), the minimum vane wall temperatures in the trailing-edge region achieved with any amount of blowing were still higher than those measured without film-cooling holes near the leading edge.

Lewis Research Center,

National Aeronautics and Space Administration,

Cleveland, Ohio, November 29, 1973,

501-24.

## APPENDIX - SYMBOLS

h	heat transfer coefficient, $W/m^2-K$ (Btu/hr-ft <sup>2</sup> -°F)
k	thermal conductivity, $W/m-K$ (Btu/hr-ft-°F)
L	total surface distance from stagnation point, cm (in.)
P	pressure, $N/cm^2$ (psia)
T	temperature, K (°F)
t	vane wall thickness, cm (in.)
V	velocity, cm/sec (ft/sec)
w	flow rate, kg/hr (lbm/hr)
x	surface distance from stagnation point, cm (in.)
$\rho$	density, $kg/m^3$ (lbm/ft <sup>3</sup> )
$\phi$	local cooling effectiveness, or temperature difference ratio

### Subscripts:

c	coolant, or coolant-side surface
e	effective
fc	film coolant
g	gas, or gas-side surface
i	inlet
mc	midchord coolant
o	with holes but without blowing
oo	without holes
w	wall
1, 2, . . . , 8	thermocouple locations

## REFERENCES

1. Yeh, Frederick C.; Gladden, Herbert J.; Gauntner, James W.; and Gauntner, Daniel J.: Comparison of Cooling Effectiveness of Turbine Vanes with and Without Film Cooling. TM X-3022, 1974.
2. Gauntner, Daniel J.: Comparison of Temperature Data from an Engine Investigation for Film-Cooled and Non-Film-Cooled, Spanwise-Finned Vanes Incorporating Impingement Cooling. TM X-2819, 1973.
3. Yeh, Frederick C.; Gladden, Herbert J.; and Gauntner, James W.: Comparison of Heat Transfer Characteristics of Three Cooling Configurations for Air-Cooled Turbine Vanes Tested in a Turbojet Engine. NASA TM X-2580, 1972.
4. Lander, R. D.; Fish, R. W.; and Suo, M.: The External Heat Transfer Distribution on Film Cooled Turbine Vanes. Paper 72-9, AIAA, Jan. 1972.
5. Gladden, Herbert J.; Gauntner, James W.; Yeh, Frederick C.; and Gauntner, Daniel J.: An Adverse Effect of Film Cooling on the Suction Surface of a Turbine Vane. NASA TM X-68210, 1973.
6. Calvert, Howard F.; Cochran, Reeves P.; Dengler, Robert P.; Hickel, Robert O.; and Norris, James W.: Turbine Cooling Research Facility. NASA TM X-1927, 1970.
7. Crowl, Robert J.; and Gladden, Herbert J.: Methods and Procedures for Evaluating, Forming, and Installing Small-Diameter Sheathed Thermocouple Wire and Sheathed Thermocouples. NASA TM X-2377, 1971.
8. Gladden, Herbert J.; Gauntner, Daniel J.; and Livingood, John N. B.: Analysis of Heat-Transfer Tests of an Impingement-Convection-and Film-Cooled Vane in a Cascade. NASA TM X-2376, 1971.
9. Anon.: High Temperature High Strength Nickel Base Alloys. The International Nickel Company, Inc. 2nd Edition, June 1968.
10. Ambrok, G. S.: Approximate Solution of Equations for the Thermal Boundary Layer with Variations in Boundary Layer Structure. Soviet Phys-Tech Phys, vol. 2, no. 9, Sept. 1957, p. 1979-1986.
11. Kays, William M.: Convective Heat and Mass Transfer. McGraw Hill Book, Inc., 1966.
12. Brown, W. Byron; and Donoughe, Patrick L.: Extension of Boundary-Layer Heat-Transfer Theory to Cooled Turbine Blades. NACA RM E50F02, 1950.

13. Brown, W. Byron; Slone, Henry O.; and Richards, Hadley T.: Procedure for Calculating Turbine Blade Temperatures and Comparison of Calculated with Observed Values for Two Stationary Air-Cooled Blades. NACA RM E52H07, 1952.
14. Dunham J.: Predictions of Boundary Layer Transition on Turbomachiner Blades. Boundary Layer Effects in Turbomachines. J. Surugue, ed., AGARD-AG-164, 1972, pp. 55-71.
15. Gladden, Herbert J.; Dengler, Robert P.; Evans, David G.; and Hippensteele, Steven A.: Aerodynamic Investigation of Four-Vane Cascade Designed for Turbine Cooling Studies. NASA TM X-1954, 1970.

TABLE I. - LOCATION OF THERMOCOUPLES

[Suction surface; total surface distance from stagnation point, L, 7.27 cm (2.861 in.).]

Thermocouple	Surface distance from stagnation point, x		Location, x/L	Vane wall thickness, t	
				cm	in.
	cm	in.			
1	6.45	2.54	0.888	0.15	0.06
2	5.83	2.295	.802	.216	.085
3	5.35	2.105	.736	.25	.10
4	4.67	1.84	.643	.29	.15
5	3.83	1.51	.528	.25	.10
6	3.00	1.18	.412	.25	.10
7	2.31	.91	.318	.25	.10
8	1.05	.415	.145	.15	.06

TABLE II. - EXPERIMENTAL DATA

Data set	Gas inlet total temperature, $T_{g,i}$ , K	Gas inlet total pressure, $P_{g,i}$ , N/cm <sup>2</sup>	Gas flow per channel, $w_g$ , kg/hr	Coolant inlet temperature, $T_{c,i}$ , K	Midchord-coolant- to gas-flow ratio, $w_{mc}/w_g$	Film-coolant- to gas-flow ratio, $w_{fc}/w_g$	$T_{w,1}$	$T_{w,2}$	$T_{w,3}$	$T_{w,4}$	$T_{w,5}$	$T_{w,6}$	$T_{w,7}$	$T_{w,8}$
							Vane wall temperature, K							
1	1286	~22.7	~1230	283	0.0461	-----	689	711	701	686	715	815	927	1168
2	1283	↓	↓	↓	.0296	-----	772	784	772	759	791	882	978	1177
3	1283	↓	↓	↓	.0162	-----	867	872	861	851	881	961	1038	1192
4	1284	↓	↓	↓	.0110	-----	930	928	918	910	937	1008	1074	1201
5	1284	↓	↓	284	.00718	-----	984	979	969	963	987	1051	1106	1210
6	1283	↓	↓	↓	.00732	0.00543	1014	1013	992	969	968	967	934	1093
7	1284	↓	↓	↓	.00740	.0102	983	980	959	924	907	893	858	1024
8	1283	↓	↓	↓	.00730	.0208	952	947	926	889	876	878	836	924
9	1284	↓	↓	↓	.00729	.0276	943	939	918	884	878	887	829	876
10	1267	↓	↓	289	.00699	.00056	998	996	983	971	986	1039	1083	1192
11	1268	↓	↓	289	.00691	.00188	1044	1043	1023	1008	1011	1026	1032	1158
12	1267	↓	↓	289	.00690	.00255	1042	1039	1021	1005	1006	1013	1009	1143
13	1268	↓	↓	288	.00685	.00361	1036	1036	1015	997	994	991	978	1124
14	1267	↓	↓	288	.00687	.00466	1031	1030	1011	991	984	976	955	1108
15	1268	↓	↓	288	.00687	.00086	1022	1013	993	976	983	1024	1060	1176
16	1269	↓	↓	289	.00705	.00564	1003	1004	983	963	958	957	924	1082
17	1275	↓	↓	288	.00706	.00556	1008	1009	988	967	963	961	928	1087
18	1276	↓	↓	↓	.00675	.00866	992	990	969	938	920	906	869	1036
19	1276	↓	↓	↓	.00695	.0126	970	967	946	908	884	871	840	984
20	1274	↓	↓	↓	.00668	.0176	958	955	933	896	876	870	836	946
21	1271	↓	↓	291	.0190	.0199	851	857	840	806	798	814	793	919
22	1266	↓	↓	290	.0190	.0152	859	863	849	813	799	806	789	957
23	1267	↓	↓	↓	.0190	.0105	876	882	868	836	823	824	805	1005
24	1262	↓	↓	↓	.0179	.00725	878	887	872	847	843	851	829	1028
25	1269	↓	↓	↓	.0180	.00497	903	912	897	877	883	900	883	1079
26	1262	↓	↓	290	.0181	.00381	902	910	898	882	891	906	907	1100
27	1272	↓	↓	289	.0182	.00251	917	925	909	896	909	932	946	1134
28	1283	↓	↓	283	.0350	.0277	755	768	759	726	734	778	758	868
29	1286	↓	↓	283	.0354	.0207	762	774	765	729	732	769	762	916
30	1287	↓	↓	284	.0353	.0114	779	793	783	747	741	763	762	983



31	1287	~22.7	~1230	283	0.0350	0.00595	803	819	809	780	788	817	809	1051
32	1268	↓	↓	291	.0351	.00056	777	784	771	751	772	851	941	1160
33	1267	↓	↓	292	.0348	.00009	746	763	757	741	767	854	952	1165
34	1263	↓	↓	↓	.0351	.00102	822	833	819	794	804	859	922	1143
35	1264	↓	↓	↓	.0350	.00152	822	838	827	808	820	863	904	1123
36	1264	↓	↓	↓	.0348	.00213	825	842	831	813	827	864	892	1116
37	1268	↓	↓	293	.0347	.00324	824	842	831	812	824	854	869	1104
38	1270	↓	↓	↓	.0345	.00405	822	840	830	810	820	847	855	1094
39	1271	↓	↓	↓	.0354	.00511	816	832	824	803	812	844	842	1080
40	1267	↓	↓	↓	.0351	.00612	804	822	812	787	792	822	812	1049
41	1268	↓	↓	↓	.0353	.00919	791	808	799	769	763	783	744	1013
42	1271	↓	↓	↓	.0354	.0139	777	791	782	748	738	757	755	966
43	1271	↓	↓	↓	.0354	.0200	765	778	770	737	733	765	759	918
44	1266	↓	↓	290	-----	.027	1079	1078	1061	1036	1011	972	885	886
45	1265	↓	↓	289	-----	.0205	1086	1083	1067	1040	1009	961	892	934
46	1266	↓	↓	288	-----	.0156	1099	1097	1079	1251	1015	958	895	976
47	1268	↓	↓	↓	-----	.0114	1119	1119	1102	1078	1044	980	917	1023
48	1267	↓	↓	↓	-----	.00697	1149	1151	1139	1126	1107	1052	986	1088
49	1267	↓	↓	↓	-----	.00474	1164	1168	1154	1148	1133	1079	1032	1125
50	1268	↓	↓	↓	-----	.00396	1170	1175	1162	1158	1146	1099	1060	1144
51	1273	~25.5	~1380	290	.0332	.0229	768	782	774	742	741	776	759	888
52	1271	↓	↓	291	.0352	.0199	760	776	768	734	729	763	752	908
53	1273	↓	↓	↓	.0356	.0139	770	786	778	743	732	752	744	952
54	1268	↓	↓	↓	.0351	.0101	781	799	789	756	746	761	749	985
55	1267	↓	↓	↓	.0349	.00701	801	820	813	784	784	810	795	1039
56	1261	↓	↓	↓	.0350	.00508	809	830	823	799	807	842	832	1069
57	1269	↓	↓	↓	.0348	.00418	815	837	828	807	817	852	851	1092
58	1268	↓	↓	↓	.0351	.00237	822	843	832	814	830	871	889	1118
59	1267	↓	↓	↓	.0349	.00113	826	845	836	817	831	879	924	1143
60	1266	↓	↓	290	.0351	.00056	816	826	805	781	793	862	938	1156
61	1267	~31.0	~1670	290	.0350	No holes	777	782	766	747	769	854	948	1163
62	1261	↓	↓	293	.0646	↓	597	629	619	609	643	740	883	1138
63	1274	↓	↓	293	.0551	↓	617	761	642	631	666	763	902	1142
64	1274	↓	↓	292	.0356	↓	692	719	709	698	737	832	952	1154
65	1277	↓	↓	292	.0303	↓	726	746	737	726	766	858	972	1162

TABLE II. - Concluded. EXPERIMENTAL DATA

Data set	Gas inlet, total temperature, $T_{g,i}$ , K	Gas inlet total pressure, $P_{g,i}$ , N/cm <sup>2</sup>	Gas flow per channel, $w_g$ , kg/hr	Coolant inlet temperature, $T_{c,i}$ , K	Midchord-coolant-to gas-flow ratio, $w_{mc}/w_g$	Film-coolant-to gas-flow ratio, $w_{fc}/w_g$	$T_{w,1}$	$T_{w,2}$	$T_{w,3}$	$T_{w,4}$	$T_{w,5}$	$T_{w,6}$	$T_{w,7}$	$T_{w,8}$
							Vane wall temperature, K							
66	1275	~31.0	~1670	291	0.0227	No holes	773	790	782	773	812	899	1001	1169
67	1281	↓	↓	290	.0175	↓	821	836	826	818	856	934	1028	1178
68	1281	↓	↓	289	.0128	↓	871	881	874	868	903	979	1058	1187
69	1282	↓	↓	289	.0104	↓	909	917	908	903	937	1008	1078	1192
70	1286	↓	↓	288	.00677	↓	971	976	968	962	991	1054	1112	1203
71	1283	↓	↓	↓	.00493	↓	1013	1014	1006	1000	1025	1083	1131	1205
72	1283	↓	↓	↓	.00130	↓	1116	1118	1112	1109	1127	1159	1181	1221
73	1283	↓	↓	↓	.00047	↓	1158	1166	1164	1172	1188	1203	1209	1227
74	1287	↓	↓	292	.0558	↓	627	662	648	637	672	771	911	1154
75	1280	↓	↓	292	.0447	↓	658	691	677	666	703	801	933	1156
76	1278	↓	↓	291	.0357	↓	697	724	711	700	738	834	957	1160
77	1276	↓	↓	290	.0279	↓	747	769	755	744	781	873	984	1166
78	1279	↓	↓	290	.0204	↓	803	819	807	798	836	921	1019	1177
79	1279	↓	↓	289	.0118	↓	889	901	891	885	919	992	1068	1189
80	1283	↓	↓	289	.00746	↓	954	962	952	948	977	1043	1104	1201
81	1268	↓	↓	292	.0509	-----	762	788	776	742	746	813	908	1162
82	1264	↓	↓	291	.0316	-----	837	849	828	797	807	877	964	1173
83	1262	↓	↓	290	.0173	-----	927	925	897	872	889	954	1025	1185
84	1264	↓	↓	289	.00869	-----	1014	1006	977	961	978	1036	1088	1202
85	1263	↓	↓	289	.00326	-----	1106	1094	1071	1057	1070	1112	1143	1211
86	1286	↓	↓	287	.00372	0.0353	1004	998	982	948	939	946	836	816
87	1286	↓	↓	↓	.00377	.0290	1013	1008	989	954	942	939	847	860
88	1287	↓	↓	↓	.00379	.0166	1031	1023	1002	957	924	901	838	955
89	1284	↓	↓	↓	.00376	.00835	1074	1068	1053	1017	992	963	896	1059
90	1283	↓	↓	286	.00374	.00359	1107	1103	1089	1063	1057	1048	999	1135
91	1283	↓	↓	↓	.00816	.00359	1021	1025	1013	987	989	997	960	1126
92	1286	↓	↓	↓	.00847	.00644	1000	1002	990	957	946	938	884	1069
93	1288	↓	↓	↓	.00840	.0128	964	962	946	903	877	860	808	983
94	1287	↓	↓	↓	.00828	.0233	940	939	924	886	876	882	819	891
95	1286	↓	↓	285	.0186	.0235	852	858	849	813	810	833	789	887

96	1288	~31.0	~1670	285	0.0185	0.0123	875	882	872	831	812	812	774	982
97	1287				.0186	.0171	862	867	857	817	802	813	779	937
98	1273				.0185	.00641	898	908	901	869	864	874	836	1052
99	1274			↓	.0185	.00433	913	923	919	891	896	918	889	1093
100	1272			289	.0185	.00171	924	939	932	908	924	959	961	1143
101	1261				.0182	.00249	914	927	922	897	908	936	923	1114
102	1260				.0182	.00301	911	924	920	894	902	926	908	1105
103	1259				.0183	.00374	905	918	912	886	890	912	884	1083
104	1259			↓	.0183	.00526	893	903	898	868	863	875	836	1046
105	1272			284	.0375	.00433	795	820	823	795	800	843	829	1082
106	1274				.0376	.00782	778	799	800	766	757	781	757	1021
107	1273				.0376	.0138	753	772	771	734	719	741	722	950
108	1278			↓	.0374	.0164	748	768	765	728	717	745	728	930
109	1278			294	.0374	.0263	736	757	757	726	729	774	742	855
110	1266			293	.0376	.00867	768	790	790	756	743	763	738	997
111	1267			293	.0377	.00590	786	811	812	782	731	815	793	1047
112	1266			293	.0378	.00394	796	821	823	796	801	844	831	1079
113	1270			292	.0376	.00307	799	827	828	800	800	852	847	1097
114	1270			292	.0374	.00199	805	832	834	807	320	871	881	1119
115	1268			292	.0376	.00138	808	834	836	809	824	879	901	1134
116	1263			285	-----	.0206	1080	1076	1059	1027	992	942	858	906
117	1263			284	-----	.0150	1094	1091	1073	1041	998	833	851	954
118	1261				-----	.0115	1111	1108	1093	1063	1023	953	867	994
119	1261			↓	-----	.00825	1135	1136	1124	1103	1073	1009	923	1046
120	1262			↓	-----	.00533	1159	1163	1153	1141	1125	1076	1001	1099
121	1273	~45.5	~2450	293	.0364	-----	817	852	861	851	855	922	969	1169
122	1274			293	.0349	.00078	819	853	860	849	851	914	941	1152
123	1276			294	.0355	.00172	813	845	853	841	839	895	901	1128
124	1278				.0355	.00235	808	842	849	836	833	883	875	1112
125	1277				.0357	.00517	792	824	827	809	795	824	792	1047
126	1282				.0354	.00957	767	794	792	768	742	753	712	963
127	1277			↓	.0355	.0152	752	778	775	749	724	740	706	911
128	1276			295	.0356	.0259	739	764	766	747	739	779	734	829

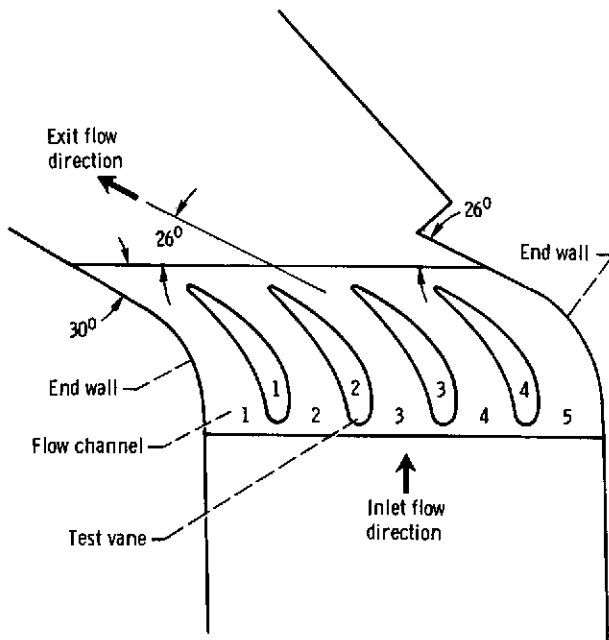
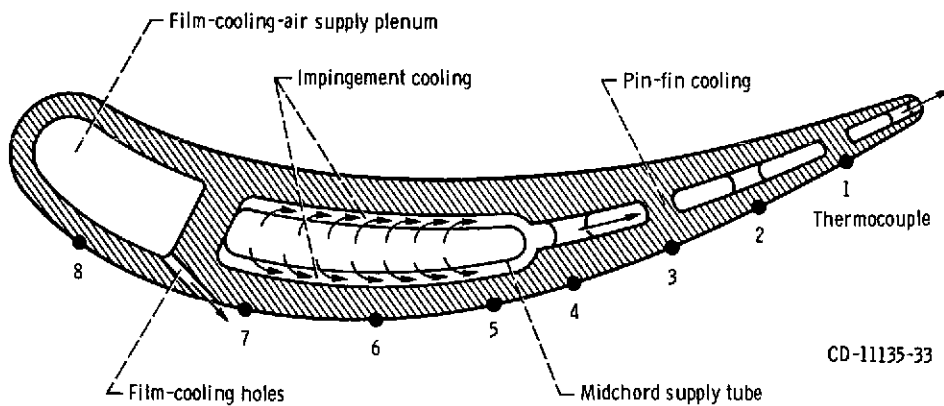
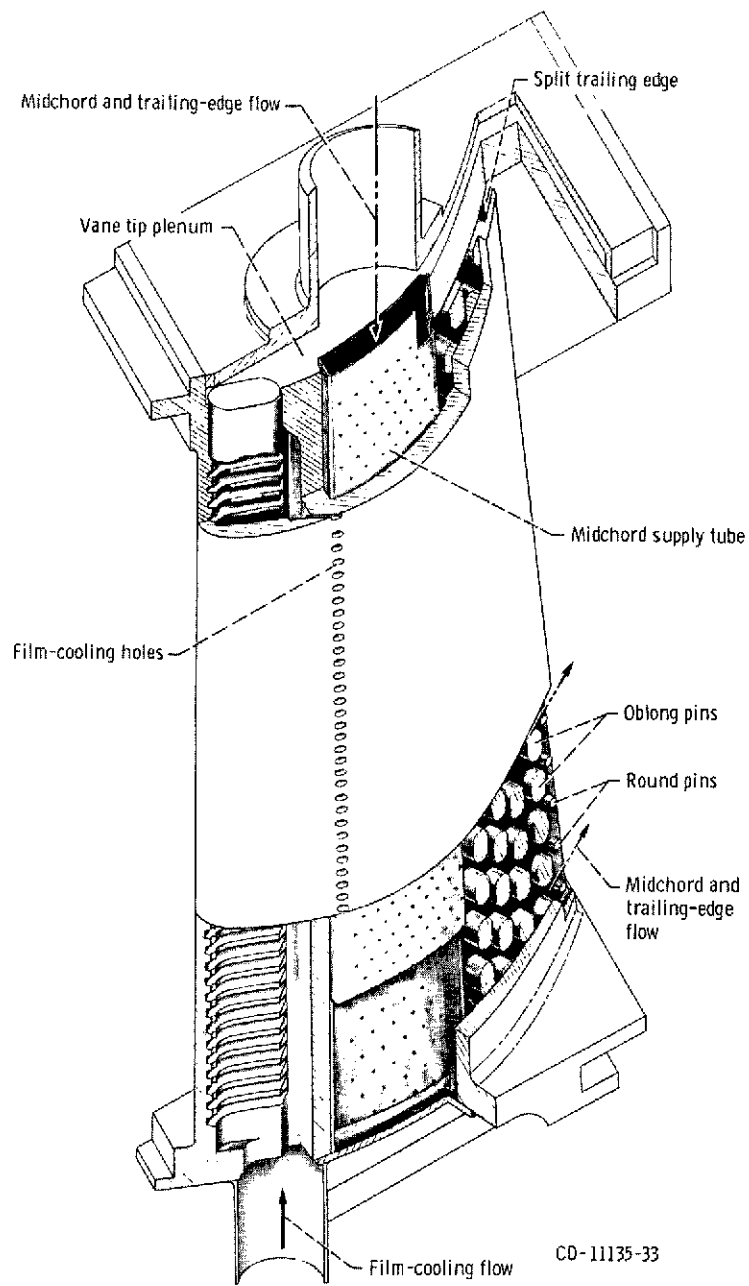


Figure 1. - Plan view of cascade test section.



(a) Cross-sectional midspan view showing internal cooling scheme and thermocouple locations.

Figure 2. - Schematic view of J-75 size test vane.



(b) Cutaway view.

Figure 2. - Concluded.

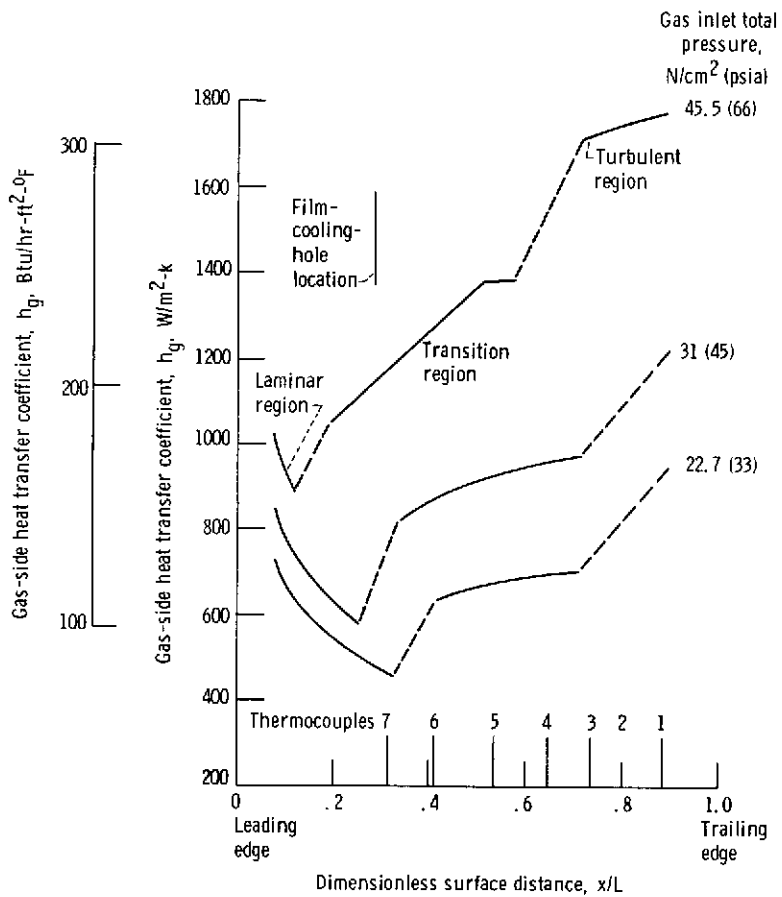


Figure 3. - Heat transfer coefficient distribution on vane midspan suction surface. Gas inlet total temperature,  $T_{g,i}$ , 1260 K (1800° F).

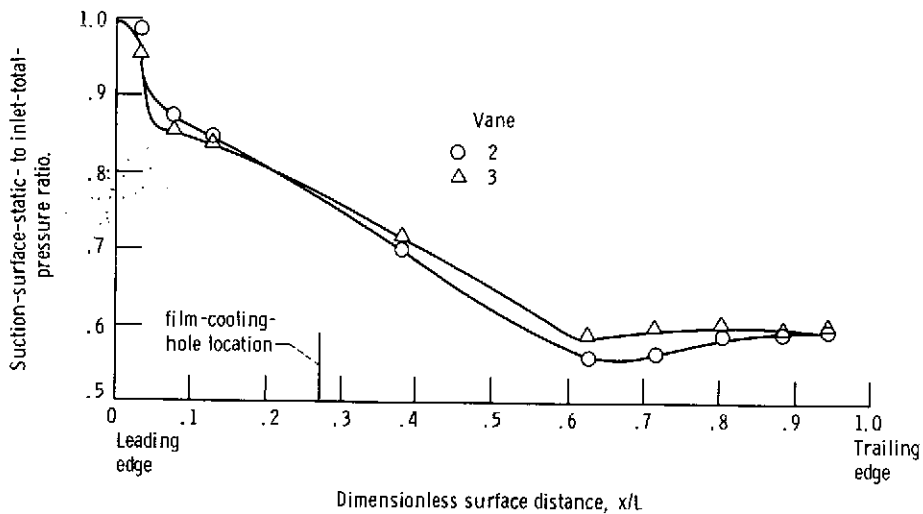


Figure 4. - Experimental midspan distribution of suction-surface-static- to inlet-total-pressure ratio at an exit Mach number of 0.85. (Data from ref. 4.)

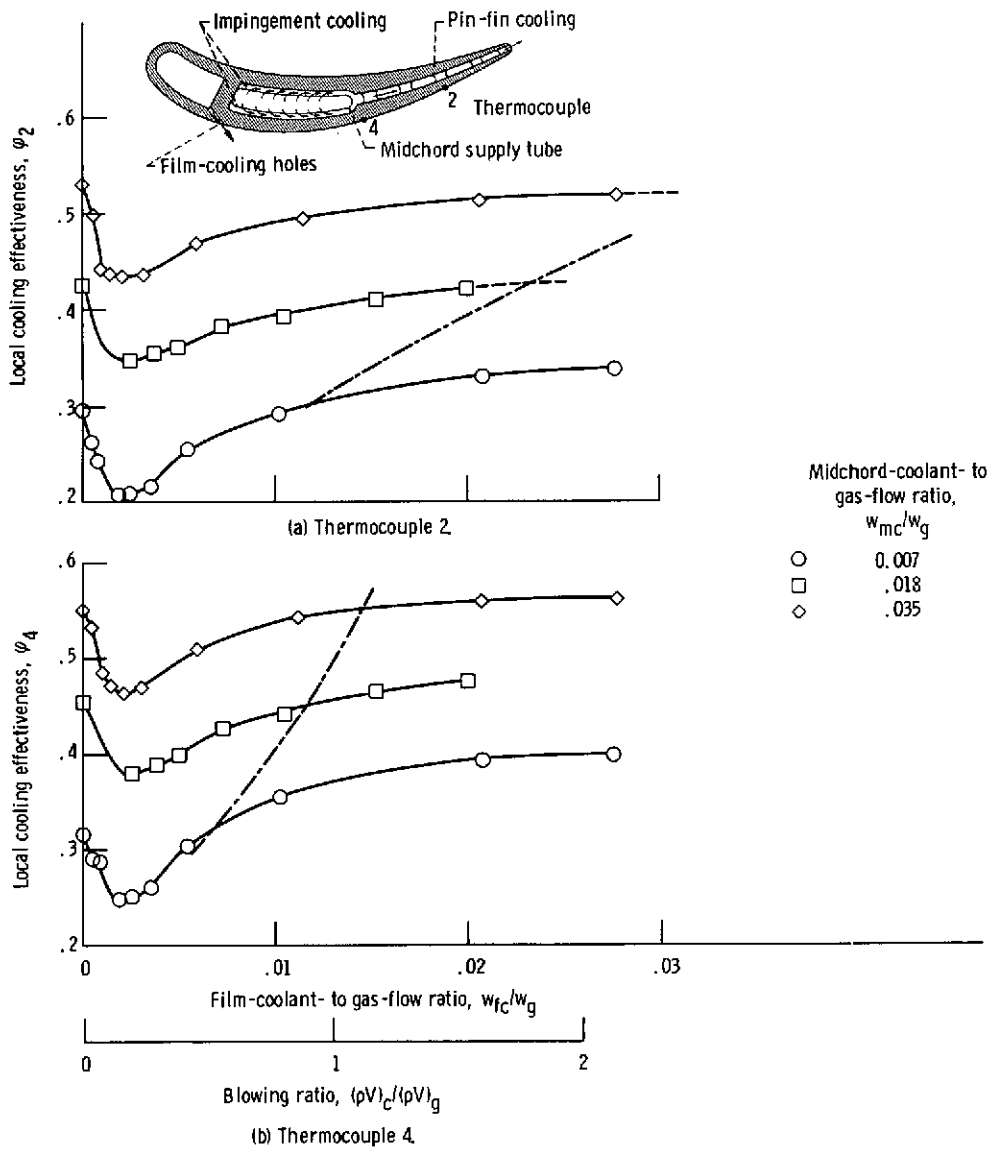


Figure 5. - Local midspan cooling effectiveness as function of film-cooling flow ratio. Gas inlet total pressure,  $P_{g,i}$ , 22.7 N/cm<sup>2</sup> (33 psia); gas inlet total temperature,  $T_{g,i}$ , 1260 K (1800° F); coolant inlet temperature,  $T_{c,i}$ , 280 K (50° F).

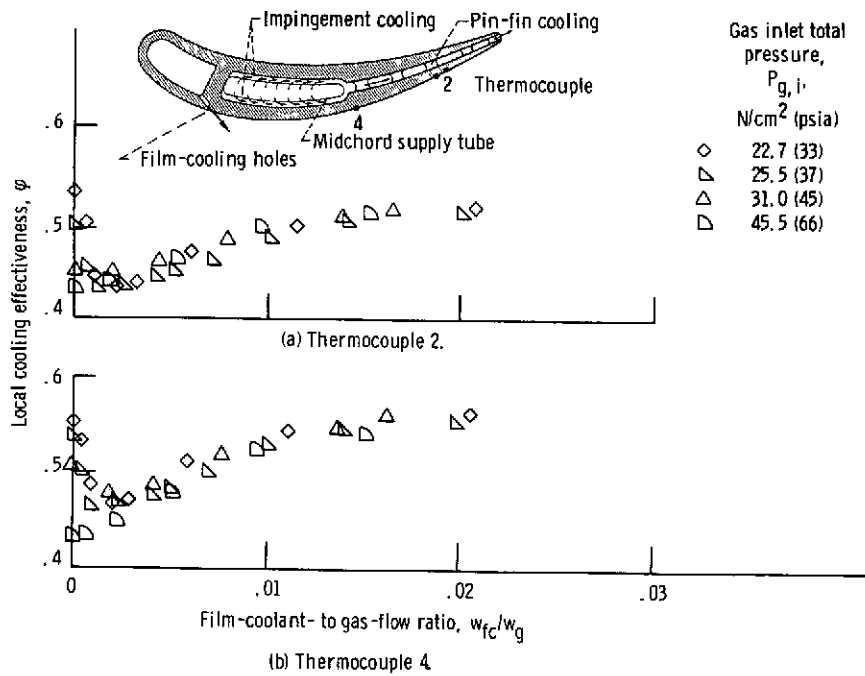


Figure 6. - Pressure effect on local midspan cooling effectiveness. Midchord flow ratio, 0.035; gas inlet total temperature,  $T_{g,i}$ , 1260 K (1800° F); coolant inlet temperature,  $T_{c,i}$ , 280 K (50° F).



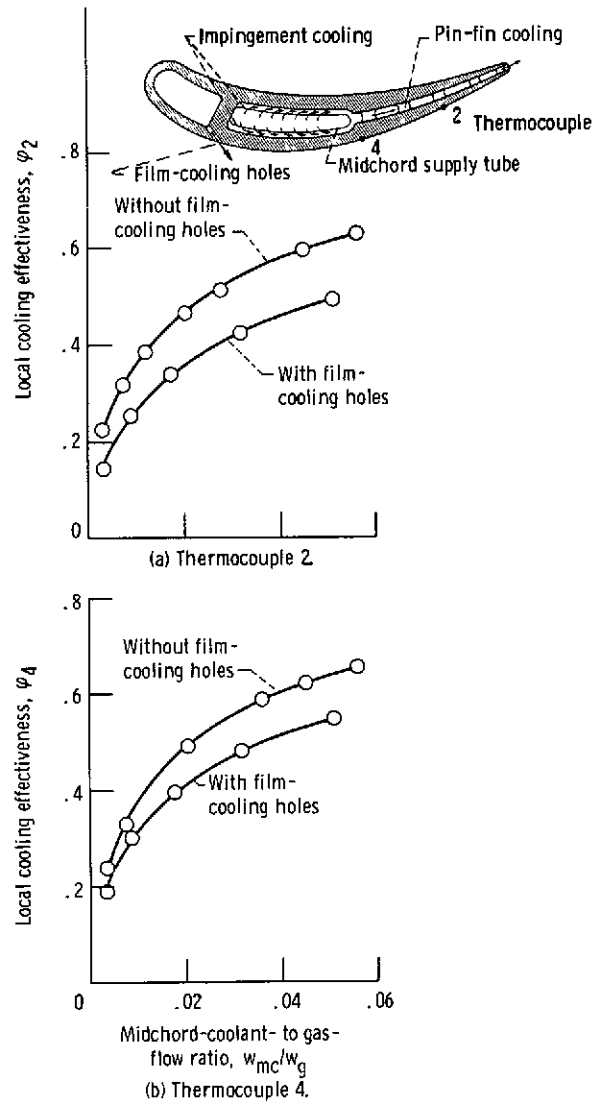


Figure 7. - Comparison of midspan cooling effectiveness with and without film-cooling holes. Gas inlet total pressure,  $P_{g,i}$ ,  $31 \text{ N/cm}^2$  (45 psia); gas inlet total temperature,  $T_{g,i}$ , 1260 K (1800° F); coolant inlet temperature,  $T_{c,i}$ , 280 K (50° F).

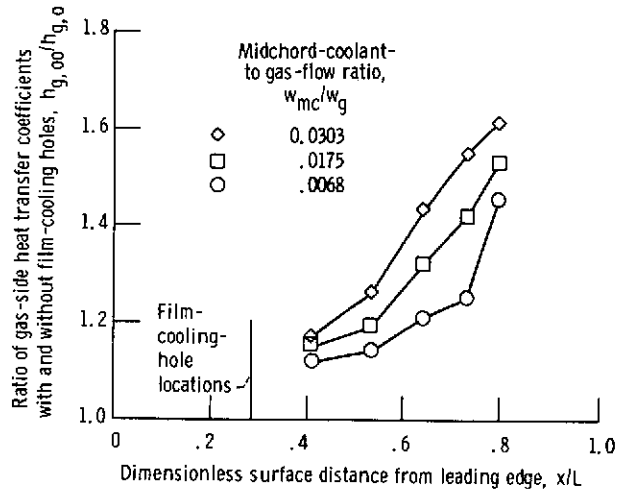


Figure 8. - Increase in gas-side heat transfer coefficients due to presence of film-cooling holes but without film-cooling flow.

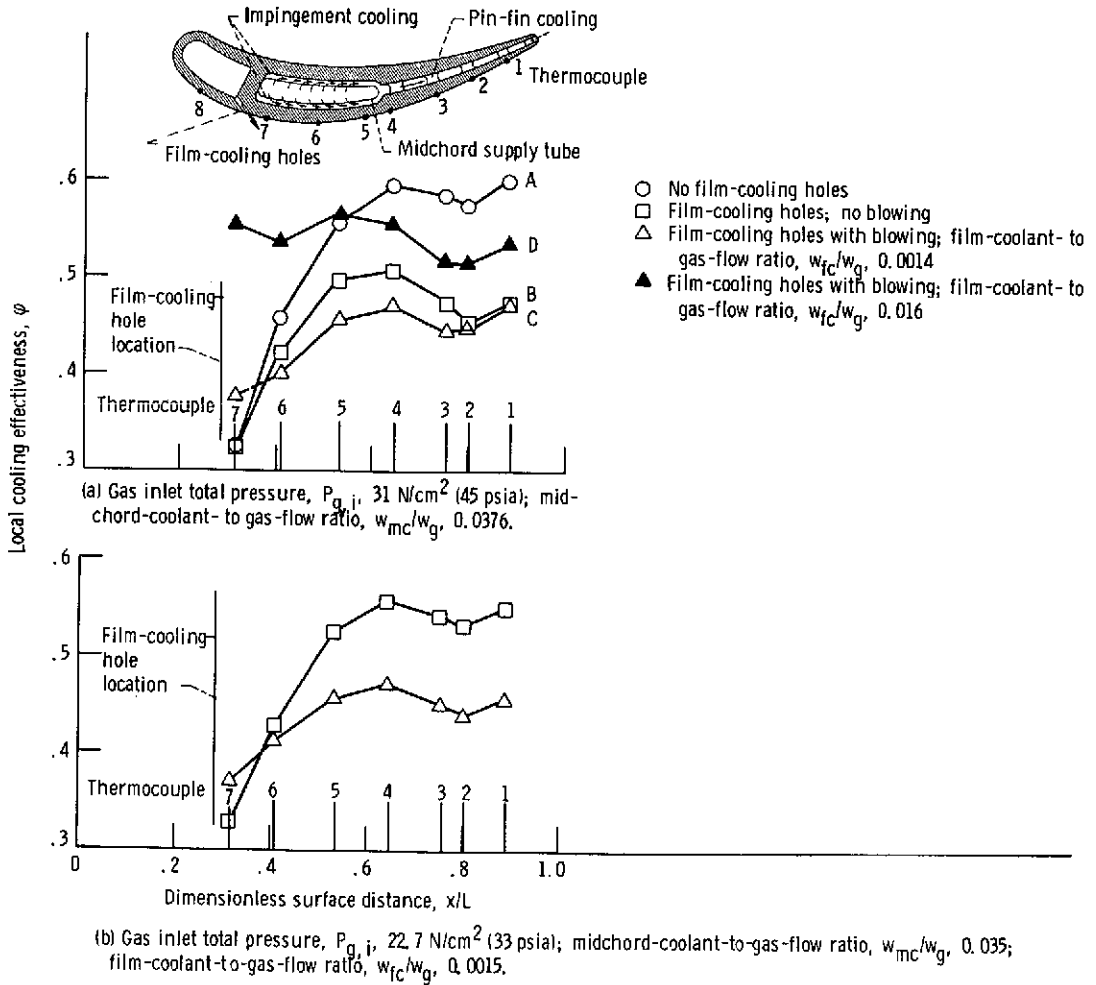


Figure 9. - Effect of film-cooling holes and blowing on vane cooling effectiveness.